Available online at www.sciencedirect.com
ScienceDirect
Bioorganic & Medicinal Chemistry 16 (2008) 313–321
Bioorganic & Medicinal Chemistry

SAR of a series of anti-HSV-1 acridone derivatives, and a rational acridone-based design of a new anti-HSV-1 3*H*-benzo[*b*]pyrazolo[3,4-*h*]-1,6-naphthyridine series

Alice M. R. Bernardino,[a,*] Helena C. Castro,[b,*] Izabel C. P. P. Frugulhetti,[b] Natália I. V. Loureiro,[b,c] Alexandre R. Azevedo,[a] Luiz C. S. Pinheiro,[a] Thiago M. L. Souza,[b] Viveca Giongo,[b] Fabiana Passamani,[c] Uiaran O. Magalhães,[c] Magaly G. Albuquerque,[d] Lúcio M. Cabral[c] and Carlos R. Rodrigues[a,c,*]

[a]*Universidade Federal Fluminense, Instituto de Química, Departamento de Química Orgânica, Programa de Pós-Graduação em Química Orgânica, Campus do Valonguinho, 24210-150 Niterói, RJ, Brazil*
[b]*Universidade Federal Fluminense, Instituto de Biologia, Departamento de Biologia Celular e Molecular, 24020-150 Niterói, RJ, Brazil*
[c]*Universidade Federal do Rio de Janeiro, Faculdade de Farmácia, ModMolQSAR, 24020-150 Rio de Janeiro, RJ, Brazil*
[d]*Universidade Federal do Rio de Janeiro, Instituto de Química, Departamento de Química Orgânica, 21949-900 Rio de Janeiro, RJ, Brazil*

Received 18 May 2007; revised 16 September 2007; accepted 19 September 2007
Available online 22 September 2007

Abstract—Herpes Simplex Virus (HSV) infections are among the most common human diseases. In this work, we assess the structural features and electronic properties of a series of ten 1-hydroxyacridone derivatives (**1a–j**) recently described as a new class of non-nucleoside inhibitors of Herpes Simplex Virus-1 (HSV-1). Based on these molecules, we applied rigid analogue and isosteric replacement approaches to design and synthesize nine new 3*H*-benzo[*b*]pyrazolo[3,4-*h*]-1,6-naphthyridine derivatives (**2a–i**). The biological and computational results of these new molecules were compared with 1-hydroxyacridones. An inhibitory profile was observed in 10-Cl substituted 3*H*-benzo[*b*]pyrazolo[3,4-*h*]-1,6-naphthyridine derivative (**2f**), which presents the same substituent at the analogous position of 1-hydroxyacridone derivative (**1b**). The structure–activity relationship (SAR) studies pointed out the 10-position next to nitrogen atom as important for the anti-HSV-1 profile in the pyrazolo-naphthyridine derivatives tested, which reinforced the promising profile for further experimental investigation. The most potent acridone and pyrazolo-naphthridine derivatives were also submitted to an in silico ADMET screening in order to determine their overall drug-score, which confirmed their potential antiviral profile.

1. Introduction

Herpes Simplex Virus (HSV) infections are among the most common human diseases.[1] Currently, there are two HSV serotypes (HSV-1 and HSV-2) that may cause oral disease, keratoconjutivitis, encephalitis, and genital infections.[2] Symptomatic or asymptomatic recurrent infections are common and maternal transmission of HSV-2 to the fetus or neonate may result in herpes infections, which are rare but severe and potentially fatal.[1–3]

Most of clinical anti-herpes virus compounds are nucleoside analogues, such as acyclovir (ACV), which is the most common drug used on treatment of HSV infections.[3,4] However, during long ACV-based treatment, drug-resistant HSV strains frequently emerge. In addition, these strains often show cross-resistance with other anti-HSV agents, such as pencyclovir and gancyclovir.[5,6] In order to manage ACV-resistant strains, other non-nucleoside analogue, such as foscarnet, have been used.[7]

Keywords: Structure–activity relationship (SAR); Acridone; Pyrazolo-naphthyridine; Antiviral agent; HSV-1; In silico ADMET screening.
* Corresponding authors. Tel.: +55 21 26292146; fax: +55 2126292135 (A.M.R.B.); tel.: +55 21 25626444 (C.R.R.); +55 21 26292294 (H.C.C.); e-mail addresses: alicerolim@globo.com; gqolice@vm.uff.br; hcastrorangel@vm.uff. br; hcastrorangel@yahoo.com.br; rangel@pharma.ufrj.br

0968-0896/$ - see front matter © 2007 Elsevier Ltd. All rights reserved.
doi:10.1016/j.bmc.2007.09.032

Nonetheless, resistance to foscarnet is also emerging, which demands new antiviral agents for HSV treatment.[6,7]

Natural and synthetic acridone derivatives have been identified as new heterocyclic systems with anti-HSV activity.[20–25] In 1989, Yamamoto and co-workers[8] reported a new acridone alkaloid, citrusinine-I (Fig. 1), which exhibited potent activity against HSV-1 and HSV-2.[8] More recently, Lowden and Bastow reported a new synthetic series of 1-hydroxyacridones with two 1,3-dihydroxyacridone derivatives showing potent HSV-1 inhibitory activity, namely, 5-methoxy-1,3-dihydroxyacridone (**1a**, ED_{50} = 2.2 μM) and 5-chloro-1,3-dihydroxyacridone (**1b**, ED_{50} = 4 ± 1 μM) (Fig. 1) .[10–12]

In this work, we used a molecular modeling approach for developing structure–activity relationship (SAR) studies on ten of these acridones (Table 1) thus we identified molecular properties important to the anti-HSV-1 activity, which may be used for designing new antiviral compounds. By using traditional medicinal chemistry principles, such as isosteric replacement and rigid analogue approaches, we designed a new potential antiviral heterocycle scaffold, namely 3*H*-benzo[*b*]pyrazolo[3,4-*h*]-1,6-naphthyridine (Scheme 1), based on two heterocycle systems, 1*H*-pyrazolo[3,4-*b*]pyridine-5-carboxylic acid, presenting a diverse antiviral profile,[13–15] and the former synthetic acridone derivatives. To investigate the impact of the isosteric aromatic ring replacement and the influence of the restricted flexibility imposed by the new naphthyridine system on the antiviral activity, nine derivatives (**2a**–**i**) from this new series (Table 2) were synthesized, tested for anti-HSV-1 effects, and evaluated in SAR studies where they were compared with

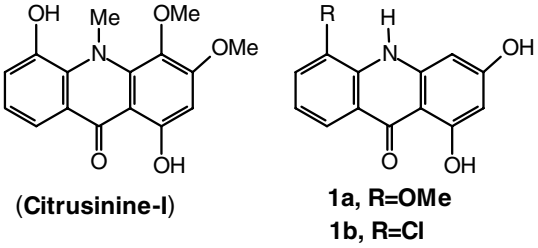

Figure 1. Structures of some acridone derivatives with anti-herpes virus activity: citrusinine-I, a natural acridone alkaloid, and two synthetic acridone derivatives **1a** (5-methoxy-1,3-dihydroxyacridone) and **1b** (5-chloro-1,3-dihydroxyacridone).

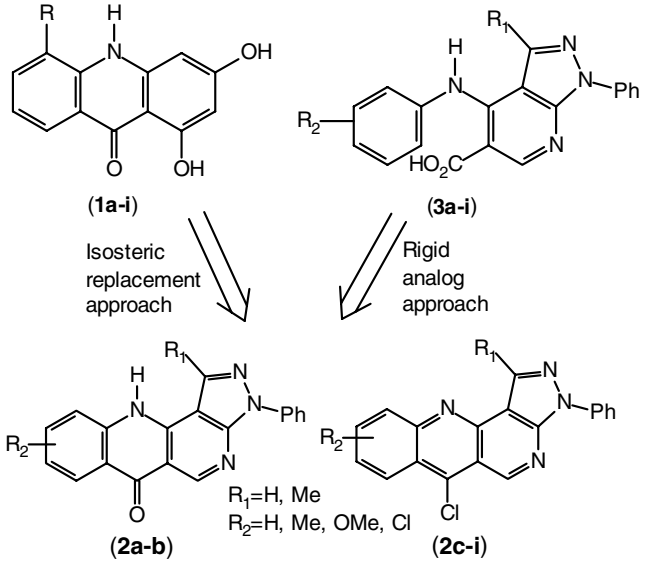

Scheme 1. Isosteric replacement and rigid analogue approaches applied into the design of the 3*H*-benzo[*b*]pyrazolo[3,4-*h*]-1,6-naphthyridine derivatives.

Table 1. Anti-HSV-1 activities (ED_{50}, μM) and the calculated HOMO (E_{HOMO}, Ev) and LUMO (E_{LUMO}, Ev) energies and molecular dipole moments (μ, Debye) of ten 1-hydroxyacridones

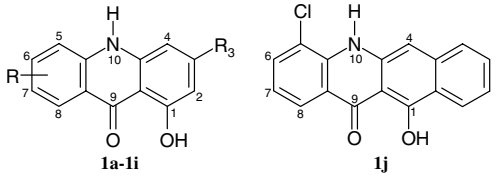

Compound	R	R_3	ED_{50}[a]	E_{HOMO}	E_{LUMO}	μ
1a	5-OMe	OH	2.2	−7.75	2.24	6.69
1b	5-Cl	OH	4 ± 1	−8.16	1.86	4.49
1c	5-Me	OH	8 ± 1	−7.89	2.19	6.53
1d	6-Cl	OH	10 ± 1	−8.22	1.88	5.84
1e	8-Cl	OH	10 ± 2	−8.06	1.95	7.56
1f	7-Cl	OH	16 ± 4	−8.06	1.86	7.62
1g	H	OH	45	−7.98	2.14	6.30
1h	5-Cl	OMe	>50(6)	−8.08	1.90	4.95
1i	5-Cl	Me	NA	−7.97	1.82	4.27
1j	[b]	[b]	NA	−7.39	1.13	2.80

NA, not active.
[a] ED_{50} values were taken from Lowden & Bastow [22]. Parenthetical value = % inhibition at stated concentration.
[b] Structure shown above.

Table 2. Anti-HSV-1 activities (HSV-1 % inhibition at 50 μM; mean ± SEM) and the calculated HOMO (E_{HOMO}, Ev) and LUMO (E_{LUMO}, Ev) energies and molecular dipole moments (μ, Debye) of nine 3*H*-benzo[*b*]pyrazolo[3,4-*h*]-1,6-naphthyridines

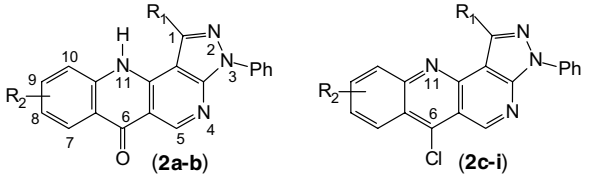

Compound	R_1	R_2	HSV-1	E_{HOMO}	E_{LUMO}	μ
2a	H	H	74 ± 2	−8.15	1.52	5.60
2b	H	8-Me	92 ± 4	−8.20	1.63	5.39
2c	H	8-Me	82 ± 1.3	−7.83	0.06	5.26
2d	H	8-OMe	68 ± 2	−7.69	0.01	5.45
2e	Me	H	70 ± 6	−7.84	0.04	4.85
2f	Me	10-Cl	100 ± 1.1	−7.91	−0.21	5.37
2g	Me	8-Cl	39 ± 3.1	−7.93	−0.19	2.47
2h	Me	10-Me	66 ± 0.8	−7.81	0.07	4.60
2i	Me	8-Me	NA	−7.75	0.08	5.44

NA, not active.

those from the 1-hydroxyacridone derivatives. Moreover, the most potent acridone and **2a–i** were submitted to an in silico ADMET screening in order to identify their promising biological potential.

2. Computational and experimental methods

2.1. Molecular modeling, SAR studies, and in silico ADMET screening

The molecular modeling study was performed using SPARTAN'04 software package (Wavefunction Inc., Irvine, CA, 2000). The minimum energy conformation of ten acridone derivatives and **2a–i** compounds was obtained by the AM1 semiempirical Hamiltonian. In order to better evaluate the electronic properties of the AM1 minimum energy conformations, they were submitted to a single-point energy ab initio calculation at the 6-311G* level.

In order to perform structure–activity relationship (SAR) studies, some electronic properties, such as HOMO (Highest Occupied Molecular Orbital) and LUMO (Lowest Unoccupied Molecular Orbital) energy values, HOMO and LUMO orbital coefficients distribution, molecular dipole moment (μ), and molecular electrostatic potential (MEP), were calculated. MEP isoenergy surface maps were generated in the range from −25.0 (deepest red color) to +30.0 (deepest blue color) kcal/mol and superimposed onto a molecular surface of constant electron density of 0.002 e/au^3. Each point of the three-dimensional molecular surface map expresses the electrostatic interaction energy value evaluated with a probe atom of positive unitary charge providing an indication of the overall molecular size and location of attractive (negative) or repulsive (positive) electrostatic potentials. The most potent acridone and the new derivatives (**2a–i**) also were submitted to an in silico ADMET screening available in http://www.acteliion.com/ or http://www.organic-chemistry.org/ to determine their overall drug-score.

2.2. Chemistry

A known synthetic approach[16–18] was used for preparing the new nine 3*H*-benzo[*b*]pyrazolo[3,4-*b*]-1,6-naphthyridine derivatives (**2a–i**), starting from two ethyl 4-chloro-1*H*-pyrazolo[3,4-*b*]pyridine-5-carboxylates (**5a–b**) as precursors (Scheme 2). Briefly, **5a–b** were prepared from 5-aminopyrazoles, through condensation with diethyl ethoxymethylenemalonate and cyclization, followed by reaction with anilines, hydrolys, and a key step of 'chlorocyclization' using phosphorus oxychloride.[18–21] **5a–b** act as good precursors for the synthesis of the present ring system due to the presence of the readily reactive 4-chloro and 5-carboxylate groups.

5a–b on fusion with several anilines led to the required ethyl 4-anilino-1*H*-pyrazolo[3,4-*b*]pyridine-5-carboxylates (**4a–i**) in good yields (56–80%). However, better results were obtained when hese reactions were carried out

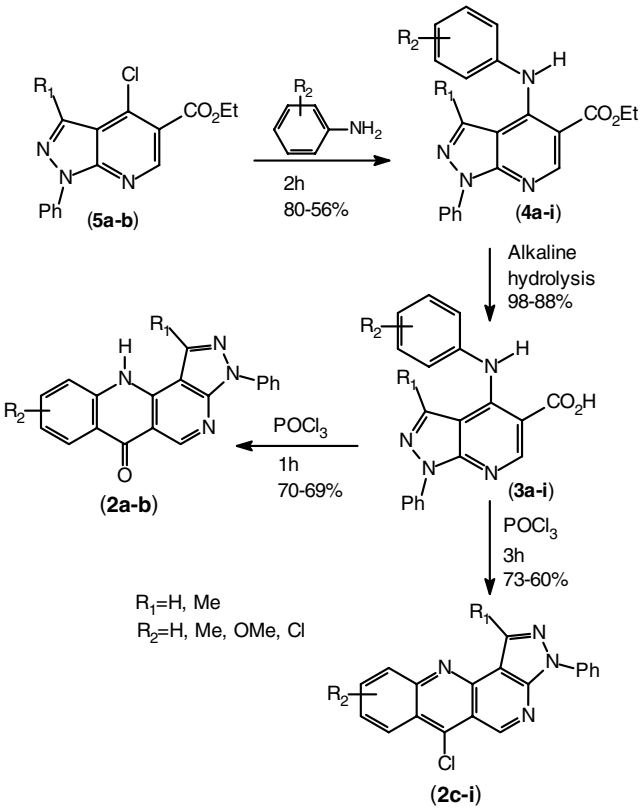

Scheme 2. Synthetic approach used to obtain the 3*H*-benzo[*b*]pyrazolo[3,4-*h*]-1,6-naphthyridine derivatives.

in solvents such as *N*,*N*-dimethylformamide.[22] Subsequently, **4a–i** were hydrolyzed to the corresponding acids (**3a–i**) (88–98%) and then cyclized to the corresponding tetracyclic heteroaromatic system (**2a–i,** 60–73%) (Scheme 2). Both 'aniline ester' (**4a–i**) and 'aniline acids' (**3a–i**) intermediates were characterized through infrared (IR) and ^{1}H nuclear magnetic resonance (^{1}H NMR) spectroscopic methods.

3. Results and discussion

3.1. Molecular modeling and SAR studies of 1-hydroxyacridone derivatives

The minimum energy conformations of **1a–j** derivatives, calculated by the AM1 semiempirical Hamiltonian, showed that, as expected, all rings of these compounds are co-planar. Subsequently, a single-point energy ab initio calculation was performed at the 6-311G* level in order to derive electronic properties, such as HOMO and LUMO energy values, HOMO and LUMO orbital coefficients distribution, molecular dipole moment (μ), and molecular electrostatic potential (MEP), which could be related to the variation of the anti-HSV-1 activity of these compounds. The SAR results showed that, although the substitution pattern into the 1-hydroxyacridone structures lead to different antiviral profile, HOMO and LUMO energy values and molecular dipole moment values did not present any direct correlation with it, as shown in Table 1.

As receptors recognize stereo-electronic effects and not atom *per se*, studies of molecular electronic properties could be very effective in interpreting the electronic structure in a comprehensive way.[21,22] Therefore, the MEP is a useful approach for understanding the electrostatic contribution for the receptor-ligand binding process.[21] The analysis of R3 position (Table 1) on MEPs generated for these compounds (Fig. 3A) revealed a negative potential (red color, i.e., negative charge) at this region when hydroxyl (**1a**–**1g**) or methoxyl (**1h**) are the substituents. However, differently of the methoxyl group (**1h**), the hydroxyl (**1a**–**1g**) may act as both donor and acceptor of hydrogen bond. In addition, methyl substituent (**1i**) or an extra aromatic ring (**1j**) has shown a reduced or absence of the negative potential in this region. This result suggested that the 3-hydroxyl group or other electron rich substituent is an important feature for reaching an anti-HVS-1 leading compound. Interestingly, presence of the 3-hydroxyl group but absence of substituents in other positions (R=H, **1g**) dramatically decreased the antiviral activity. Thus, this result points to other functional groups at C5, C6, C7, and 8 positions (R substituent, Table 1) as important for conserving a significant biological profile. Chlorine substituent at C5 (**1b**), C6 (**1d**), C7 (**1f**), and C8 (**1e**) position is somehow important for the biological profile (Table 1). However, the presence of methoxyl group (**1a**) increased the electronic density of the MEP represented by intense red color in the ring system (Fig. 3A). This feature could be involved in the 2- to 8-fold increase of **1a** derivative antiviral activity when compared to **1b** and **1c** (Fig. 3A, Table 1).

Importantly, the positive potential (blue color, i.e., positive charge) observed on MEP maps corresponding to the C4 and N10 hydrogen atom positions decreased for **1h**–**j** derivatives. Therefore, the lower or loss of the antiviral activity for **1h**–**1j** derivatives could be probably due to a clear reduction of the positive potential of these hydrogen atoms (Fig. 3A). Then, based on these SAR results and the structural features observed, we designed the nine 3*H*-benzo[*b*]pyrazolo[3,4-*h*]-1,6-naphthyridine derivatives (**2a**–**i**).

3.2. New series: 3H-benzo[*b*]pyrazolo[3,4-*h*]-1,6-naphthyridines

3.2.1. Design. **2a**–**i** derivatives were designed combining isosteric replacement and rigid analogue approaches based on two heterocycle systems, 1*H*-pyrazolo[3,4-*b*]pyridine-5-carboxylic acid presenting anti-HSV-1 activity among a diverse antiviral profile[13,14,21] and synthetic 1-hydroxyacridone derivatives with anti-HSV-1 activity. Scheme 1 shows that the acridone motif is a classical isostere of the 3*H*-benzo[*b*]pyrazolo[3,4-*h*]-1,6-naphthyridine aromatic system, while the ring closure of the 1*H*-pyrazolo[3,4-*b*]pyridine-5-carboxylic acid system leads to the 3*H*-benzo[*b*]pyrazolo[3,4-*h*]-1,6-naphthyridine motif corresponding to the rigid analogue approach.

As a result, considering the unchanged scaffold of acridone system, the N10-H and C9-carbonyl groups of acridone ring are maintained in derivatives **2a**–**b** as N11-H and C6-carbonyl groups of naphthyridinone ring, respectively. Meanwhile for **2c**–**i** derivatives, we changed the hydrogen-bonding donor (N10-H of acridone) to an acceptor (N11 of naphthyridine) character at the former position, and from C9-carbonyl group of acridone ring to C6-chlorine groups of naphthyridine ring. The C1-hydroxyl group of acridone ring has no counterpart in the naphthyridinone (**2a**–**b**) or naphthyridine (**2c**–**i**) rings, although C1-hydroxyl is close to N4 of naphthyridine ring, allowing the same hydrogen bonding acceptor capability (Scheme 1). However, according to Lowden and Bastow, removal and/or replacement of the C9-carbonyl and/or the C1-hydroxyl groups is a desirable approach, since these motifs may be responsible for cell toxicity.[9]

Therefore, we designed **2a**–**i** derivatives with R1 and R2 substituents (Scheme 1 and Table 2) to identify the role of some structural features, such as the electronic properties, to the antiviral profile. The R1 position of **2a**–**i** derivatives has no counterpart in the acridone system, so hydrogen or methyl group could be used as substituents. On the other hand, the R2 position corresponds to the C5-, C6-, C7- or C8-substituent of acridone ring, and it could be hydrogen, methyl, methoxyl, or chlorine at C10 or C8 positions of the **2a**–**i** derivatives.

3.2.2. Chemistry. The nine derivatives (**2a**–**2i**) were synthesized in good yields (60–73%) using a brief scalable and easy procedure (Scheme 2).[22] The substitution pattern is similar to that of *N*-phenylpyrazole and 1*H*-pyrazolo[3,4-*b*]pyridine and indazole. Ring system, where the free position of the pyrazole is the condensed ring, is reactive toward electrophilic substitution reaction. The products **2a** and **2b** have been represented here in the 'oxo' rather than the 'hydroxy' tautomer in accordance to that reported for such related system.[17] The infrared spectra of the compounds obtained after cyclization reaction showed a broad absorption band in the region assigned to *NH* frequency of 3400 cm^{-1} for **2a**–**b** and 3430 cm^{-1} for **2c**–**i** derivatives due to the N11 protonation. The carbonyl absorption was observed between 1620 and 1720 cm^{-1}, which also indicated the predominance of 'oxo' tautomer (**2a**–**b**). Therefore, the C9-carbonyl group of the acridone system corresponds to the C6-carbonyl group of the **2a**–**b** compounds and to the C6-chlorine of the **2c**–**i** derivatives.

3.2.3. Antiviral and cytotoxicity assays. In order to evaluate the biological profile of **2a**–**2i** derivatives, we tested them as potential inhibitors of HSV-1 replication in cell culture as described on Experimental section (Table 2). Among all compounds evaluated, derivative (**2f**) with chlorine atom at 10-position (R2=10-Cl, Table 2), structurally analogous to acridone **1b**, exhibited a high anti-HSV-1 activity (100%). In contrast, the derivative **2i** (Fig. 3B) with methyl group at 8-position did not show any inhibitory activity. Neither substituents in R1 (H or CH_3) nor in C6- (chlorine or carbonyl) positions completely abolished the antiviral activity, which reveals R2 position as the most important determinant for these

compounds' antiviral profile (Table 2). Apparently, position in the ring (10 or 8) is one of the most important structural features to be considered in R2 as **2f** and **2h** (10-substituents) presented higher activity than its analogous **2g** and **2i** (8-substituents) (Table 2).

To verify the cytotoxicity profile of this naphthyridine series, we also performed cytotoxicity assays using Vero cells. Our results showed that active and inactive derivatives present a cytotoxic concentration higher (CC_{50} = 640–4258 μM) than acyclovir (CC_{50} = 126 μM) (Fig. 2). Thus these data indicated the low cytotoxicity profile of this naphthyridine series whereas reinforced their antiviral activity.

3.2.4. Molecular modeling and SAR studies of 2a–i derivatives. The same molecular modeling procedure used for acridones was applied for the nine 3*H*-benzo[*b*]pyrazolo[3,4-*h*]-1,6-naphthyridine derivatives. The minimum energy conformation for all compounds shows that the N3-phenyl ring is co-planar to the pyrazolo-naphthyridine system probably due to the electrostatic attraction between the *ortho*-hydrogen atoms of N3-phenyl ring and the N2 and N4 nitrogen atoms of the pyrazolo-naphthyridine system (Scheme 1, Table 2, and Fig. 3B). The overall analysis of naphthyridines' calculated electronic properties, such as HOMO and LUMO energies and molecular dipole moment values, showed no clear or direct correlation with anti-HSV-1 activity, similar to that observed for acridones (Table 2).

Analysis of the MEP maps of **2a**–**i** derivatives (Fig. 3A) showed significant changes in C6-position of naphthyridine moiety in **2a** and **2b** compounds (carbonyl group) in contrast with compounds **2c**–**i** (chlorine substituent). However, since there are compounds with almost equivalent activity with carbonyl (**2b**, 100%) or chlorine (**2f**, 92%) at C6-position (Table 2), the electrostatic potential is not the determinant factor for the activity at this position, which is related to the C9-carbonyl group in acridone derivatives. This result suggested that this region might be important for the activity observed due to its hydrophobic character rather than its ability as a hydrogen-bonding acceptor. Moreover, since Lowden and Bastow have proposed the removal and/or replacement of the C9-carbonyl and/or the C1-hydroxyl groups of acridone system in order to decrease cell toxicity,[9] we designed a new series that does not contain these motifs simultaneously.

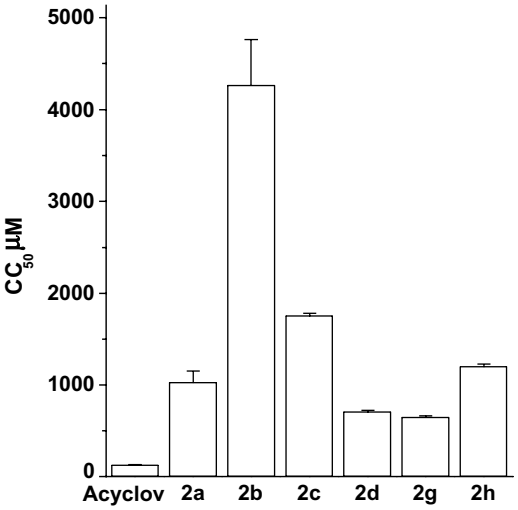

Figure 2. Comparison of the cytotoxicity concentration (CC_{50}) of active and inactive naphthyridine compounds and acyclovir (Acyclov).

The comparison of the theoretical results of (**2f**) and (**2g**) derivatives revealed that electronic density significantly decreases in the last compound when chlorine atom is in 8-position (Table 2, Fig. 3A). Probably loss of this negative region may be deleterious for **2g** binding to receptor/target of the virus, in contrast to **2f** (10-substituted derivative) as observed in the biological assays.

The comparison of the MEP energy isosurface maps of the acridone (**1a**–**g**) and naphthyridine (**2a**–**i**) derivatives (Fig. 3A) showed the highest negative electrostatic potentials close to R3=OH substituent in acridone analogues and to the N2 in naphthyridine derivatives. In fact, the three-dimensional MEP maps in both compound series reveal that the center of the most negative region (darkest red) lies near to these substituents. The structural alignment of the most active (**2f**) and the inactive (**2i**) compounds with acridone **1b** infers a restrictive role for the positions analyzed (Fig. 3B).

Despite the interesting results, it is important to consider the limitation of ligand-based SAR design when using cell-based assay data, especially when the target/mechanism of action are unknown. In case of acridone series (**1**), it is known that the mechanism of two regioisomers (**1f** and **1h**) is different, which suggests they act on different targets.[22] This may partially explain the absence of direct correlation between some calculated electronic parameters and molecular dipole moments, and the biological activity (Table 1). Thus the fact that the target/mechanism of the naphthyridine compounds studied herein is also not fully understood limits the interpretation of the computational approach used and this should be considered.

3.2.5. In silico ADMET screening. Currently, there are many approaches to assess drug-likeness and/or lead-likeness of drug candidates.[23,24] One of such approaches is the Actelion Property Explorer (http://www.actelion.com/ or http://www.organic-chemistry.org/), a web-based system named Osiris, which is able to calculate indices and/or properties such as toxicity risk assessment, logP prediction, solubility (logs) prediction, molecular weight, fragment-based drug-likeness prediction, and overall drug-score. The overall drug-score combines drug-likeness, cLogP, clogs, molecular weight, and toxicity risk indices in one single value, where the occurrence frequency of each fragment is determined within the collection of traded drugs and within the supposedly non-drug like collection of Fluka compounds.

In this work, we used the Osiris Property Explorer for calculating the overall drug-score of the most active acridone (**1a** and **1b**) and **2b, 2c,** and **2f** compounds

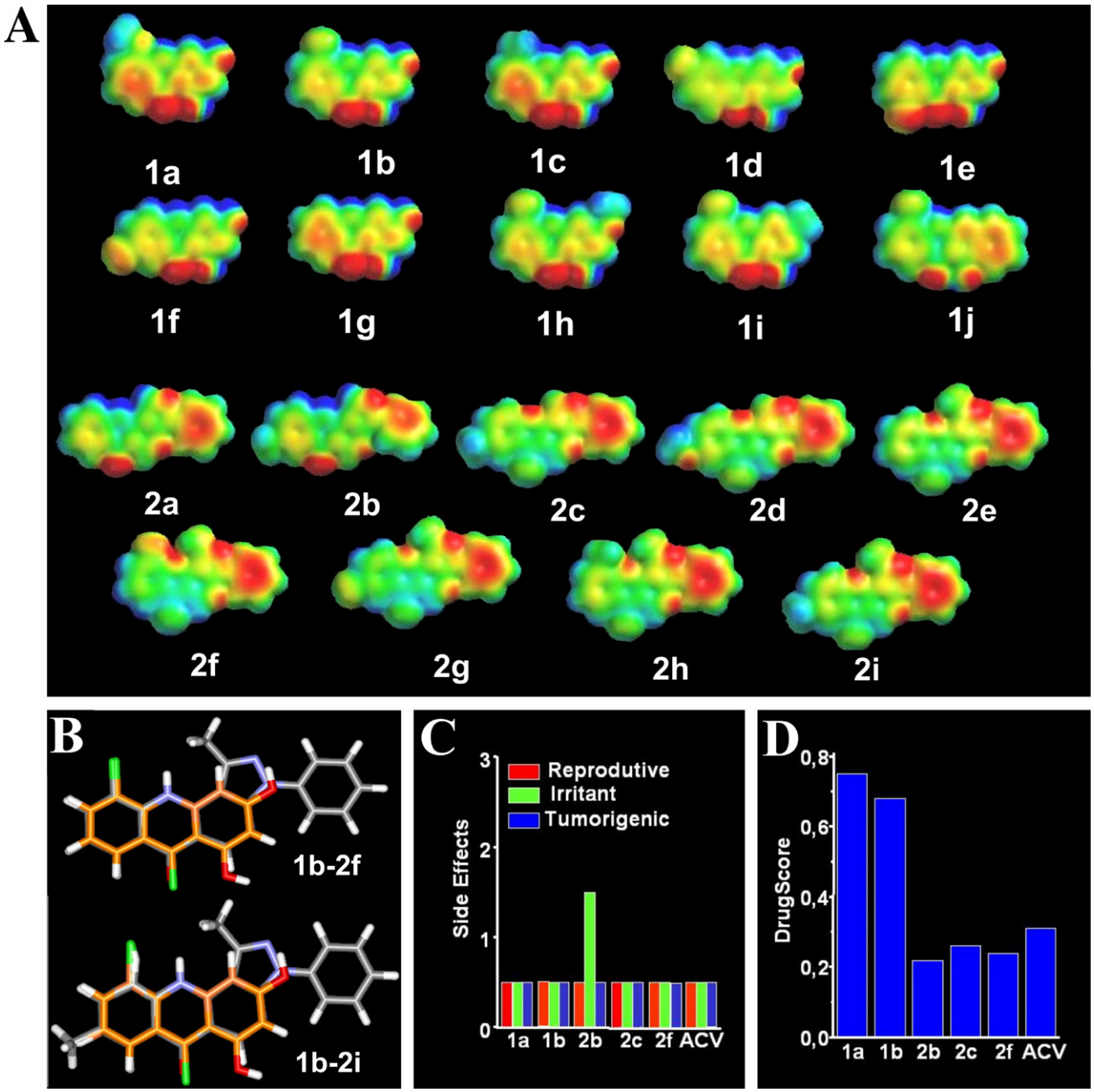

Figure 3. Theoretical studies of acridones and naphthyridines. (A) Comparison of the Molecular Electrostatic Potential (MEP) energy isosurfaces of 1-hydroxyacridones (up) and 3*H*-benzo[*b*]pyrazolo[3,4-*h*]-1,6-naphthyridines (down) superimposed onto total electron density of 0.002 e/a.u.3. The color code is in the range of −25 (deepest red) to +30 (deepest blue) kcal/mol. (B) Structural alignment of 5-chloro-1,3-dihydroxyacridone (carbon atoms are in orange color) (**1b**) with the most active (**2f**) and the inactive (**2i**) 3*H*-benzo[*b*]pyrazolo[3,4-*h*]-1,6-naphthyridine derivatives (carbon atoms are in gray color). (C) Calculated side effects (i.e., reproductive, irritant, and tumorigenic theoretical toxicity risks) and (D) calculated DrugScore values for the most potent compounds (**1a**, **2b**–**c**, and **2f**) and acyclovir (ACV) using Osiris program (http://www.organic-chemistry.org/prog/peo/druglikeness.html).

using acyclovir (ACV) as positive control as described elsewhere.[23,24] Potential toxicity risks including reproductive, irritant, and tumorigenic effects are shown in Figure 3C while the overall drug-score is shown in Figure 3D. Interestingly, **2b, 2c,** and **2f** derivatives presented a drug-score similar to acyclovir, while the acridone compounds presented a greater drug-score (Fig. 3D). Importantly, only **2b** presented the worst prediction of one of these toxicity risks (Fig. 3C). The predicted irritant profile of **2b** is a direct indication of its non-potential drug-score. The low theoretical reproductive, irritant, and tumorigenic effects of the other compounds (**1a, 1b, 2c**, and **2f**) indicated a low risk drug like profile; similar to acyclovir that in the analyzed aspects was also safe. It is important to notice that the toxicity predicted herein neither is a fully reliable toxicity prediction, nor guarantee that these compounds are completely free of any toxic effect. However it reinforced the promising profile of these compounds for further experimental investigation.

4. Conclusions

Overall in both acridones and **2a**–**i** compounds, the position of functional groups has impact on the activity as observed in the SAR study. The structure activity-relationship of acridone derivatives shows that the 5-chloro position is interesting for displaying an anti-HSV-1 rofile. Similar feature was observed in **2a**–**i** compounds, in which the highest inhibitory activity is noticed when the chloride atom is in the 10-position next to nitrogen atom of central ring.

Our results with acridones and **2a**–**i** compounds pointed their electrostatic features and other electronic properties as important in the antiviral profile. Although the Osiris risk alerts are not a fully reliable toxicity prediction, the theoretical low-toxicity profile of these compounds reinforces the significant activity of **2c** and **2f**. This theoretical result is reinforced by the experimental cytotoxicity assay, which confirmed these compounds' low toxicity profile. Therefore, the analyses of other molecular properties could be useful for designing new anti-HSV-1 drugs using some of these derivatives such as **2f** as a leading compound.

5. Experimental

5.1. Chemistry

All reagents and solvents used were of analytical grade. TLC was carried out using silica gel F-254 Glass Plate (20×20 cm). The solid samples were measured using potassium bromide pellets. Melting points (mp) were determined with a Fisher–Johns apparatus. The ^{1}H Nuclear agnetic Resonance (^{1}H NMR) spectra were obtained from Varian model Unity Plus spectrometer operating at 300.00 MHz, using tetramethylsilane as internal standard. The chemical shifts (*d*) are reported in ppm and the coupling constants (*J*) in Hertz. Fourier transform infrared (FT-IR) absorption spectra were recorded in a Perkin-Elmer model Spectrum One FT-IR spectrophotometer.

3*H*-Benzo[*b*]pyrazolo[3,4-*h*]-1,6-naphthyridines and the intermediate 'aniline esters' and 'aniline acids' were prepared as follows.

5.1.1. Ethyl 4-chloro-1-phenyl-1*H*-pyrazolo[3,4-*b*]-pyridine-5-carboxylate (5a) and Ethyl 4-chloro-3-methyl-1-phenyl-1*H*-pyrazolo[3,4-*b*]pyridine-5-carboxylate (5b). These were prepared according to literature method: (**5a**), mp 98 °C (mp 97 °C); (**5b**), mp 110 °C (mp 110 °C). [16]

5.1.2. Ethyl 4-anilino-1-phenyl-1*H*-pyrazolo[3,4-*b*]-pyridine-5-carboxylate (4a–i). Method A: An equimolar mixture of **5a** or **5b** and an aniline (5 mmoles) in 10 ml *N*,*N*-dimethylformamide was heated under reflux for 4 h. The reaction mixture, after cooling, was poured into 50 ml of ice cold water. The precipitated 'aniline esters' were filtered, dried, and recrystallized from a mixture of ethanol and water.

5.1.3. 4-Anilino-1-phenyl-1*H*-pyrazolo[3,4-*b*]-pyridine-5-carboxylic acids (3a–i). A mixture of 3 mmoles of the ester (**4a**–**i**), 10 ml of 20% sodium hydroxide solution, and 10 ml of ethanol was heated under reflux for 1–3 h. On cooling mixture was acidified with diluted hydrochloric acid (1:3), and the precipitated acids were filtered and recrystallized from a mixture of DMF and water.

5.1.4. 3-Phenyl-3*H*-benzo[*b*]pyrazolo[3,4-*h*]-1,6-naphthyridines (2a–i). A mixture of the 'aniline acids' (**3a**–**i**) and phosphorus oxychloride (5 mL) was heated under reflux for 3 h. The reaction mixture was inverted over crushed ice. In some cases the excess of phosphorus oxychloride was removed under reduced pressure before inverting over crushed ice and neutralized with water. The resulting precipitate was collected and purified by flash column chromatography (FC, silica gel).

(**2a**) *3-Phenyl-3H-benzo[b]pyrazolo[3,4-h]-1,6-naphthyridin- 6(11H)one*. Yield: 70%; mp 258 °C; IR (KBr, cm^{-1}): (*v*NH3400, *v*C=O 1650–1640); ^{1}H NMR: 6.01(s); 8.94(s); 7.84–7.47(m).

(**2b**) *3-Phenyl-8-methyl-3H-benzo[b]pyrazolo[3,4-h]-1,6-naphthyridin-6(11H)one*. Yield: 69%; mp >300 °C; IR (KBr, cm^{-1}): (*v*NH3400, *v*C=O 1650–1640); ^{1}H NMR: 6.22(s); 9.08(s); 7.51–7.28(m).

(**2c**) *6-Chloro-3-phenyl-8-methyl-3H-benzo[b]pyrazolo-[3,4-h]-1,6-naphthyridine*. Yield: 68%; mp 231 °C; IR (KBr, cm^{-1}): (*v*NH3430, *v*C=C 1593, *v*C=N 1502); ^{1}H NMR: 6.22(s); 9.19(s); 7.77(s); 7.45(dd. 7.8; 7.8); 8.11(d. 7.5); 8.33(d. 7.8); 7.28(d. 7.2); 7.02(d, 7.5); 2.51(s).

(**2d**) *6-Chloro-3-phenyl-8-methyl-3H-benzo[b]pyrazolo[3,4-h]-1,6-naphthyridine*. Yield: 70%; mp 245 °C; IR (KBr, cm^{-1}): (*v*NH3430, *v*C=C 1593, *v*C=N 1502); ^{1}H NMR: 6.70(s); 9.62(s); 7.59–7.50(m); 8.12(d, 9.3); 8.22(d, 7.8); 7.37(d, 7.5); 4.01(s).

(**2e**) *6-Chloro-3-phenyl-1-methyl-3H-benzo[b]pyrazolo-[3,4-h]-1,6-naphthyridine*. Yield: 60% mp 195–96 °C; IR (KBr, cm^{-1}): (*v*NH3430, *v*C=C 1596, *v*C=N 1502); ^{1}H NMR: 9.58(s); 8.20(d, 9.0); 7.88–7.52(m); 8.17(d, 9.0).

(**2f**) *6,10-Dichloro-3-phenyl-1-methyl-3H-benzo[b]pyrazolo[3,4-h]-1,6-naphthyridine*. Yield: 71%; mp 224 °C; IR (KBr, cm^{-1}): (*v*NH3430, *v*C=C 1596, *v*C=N 1502); ^{1}H NMR: 9.06(s); 7.81–7.48(m); 8.35(d, 8.1); 7.73(d, 8.1); 7.53(d, 7.2); 1.39(s).

(**2g**) *6,8-Dichloro-3-phenyl-1-methyl-3H-benzo[b]pyrazolo[3,4-h]-1,6-naphthyridine*. Yield: 68%; mp 243 °C; IR (KBr, cm^{-1}): (*v*NH3430, *v*C=C 1596, *v*C=N 1502); ^{1}H NMR:9.43(s); 7.93(s); 7.85(d, 7.8); 8.05(d, 7.8); 8.36(d, 7.5); 7.74(d, 7.8); 7.52(d, 7.8); 1.38(s).

(**2h**) *6-Chloro-3-phenyl-1,10-dimethyl-3H-benzo[b]pyrazolo[3,4-h]-1,6-naphthyridine*. Yield: 67%; mp >300 °C; IR (KBr, cm^{-1}): (*v*NH3430, *v*C=C 1596, *v*C=N 1502); ^{1}H NMR: 9.18(s); 7.76(s); 8.11(d, 8.0); 7.45(dd, 8.0); 8.33(d, 7.8); 7.52(dd, 7.5; 7.5); 7.28(dd, 7.5; 7.5); 2.51(s); 1.37(s).

(**2i**) *6-Chloro-3-phenyl-1,8-dimethyl-3H-benzo[b]pyrazolo[3,4-h]-1,6-naphthyridine*. Yield: 73%; mp 201 °C; IR (KBr, cm^{-1}): (νNH3430, νC=C 1592, νC=N 1503); ^{1}H NMR: 9.54(s); 8.05(d, 4.5); 7.63(dd, 9.0); 8.03(d, 9.0); 8.20(d, 7.5); 7.55(d, 7.8); 7.36(d, 7.5); 3.07(s); 1.30(s).

5.2. Antiviral assay

African green monkey kidney cells (Vero) were cultured in Dulbecco's modified Eagle's medium (DMEM; GIBCO/BRL) supplemented with 5% fetal calf serum (FCS), 100 U/mL penicillin, 100 μg/mL streptomycin, and 250 μg/mL amphotericin-β. The cells were incubated at 37 °C in a 5% CO_2 atmosphere. As the cells became confluent, they were washed with PBS-EDTA, dissociated with trypsin 0.25%, and then resuspended in culture medium. Monolayers in 25 cm^2 bottles were infected by acyclovir-resistant strain of HSV-1 (AR-29) at 0.1 multiplicity of infection (m.o.i.). Next, cells were lysed 24 h after infection by three cycles of freezing and thawing, centrifuged at 3000 rpm at 4 °C for 20 min, and the supernatant was stored at −70 °C for use.

The antiviral activities of the 3*H*-benzo[*b*]pyrazolo-[3,4-*h*]-1,6-naphthyridine derivatives (50 μM) were investigated according to Reed and Munch 50% end point method.[25] Acyclovir was used as positive control at 50 μM (HSV = 100%). Briefly, Vero cells grown to confluence in 96-well plate were infected with HSV-1 at various m.o.i. (1, 0.1, 0.01, 0.001) for 1 h at 37 °C. After that, infected cells were washed with PBS to remove residual viruses and complete culture medium, containing or not the derivatives, was added. At 72 h after infection virus titer of each sample was determined in terms of the 50% tissue culture dose (TCID 50/mL) by end point dilution. In addition we also used Mock-treated HSV1-infected cells as positive control. All experiments were performed in duplicate at least three times. Thus we presented the compounds results by using the formula $y = (100.T/M) - 100$ where y is the inhibition (%), T is the titer of the HSV-1-infected cells treated with the naphthyridine compound, and M is the titer of the Mock-treated HSV1-infected cells.

5.3. Cytotoxicity assay

Vero cells were cultured in Dulbecco's modified Eagle's medium (DMEM) supplemented with 5% fetal bovine serum (FBS; HyClone, Logan, Utah), 100 U/mL penicillin, and 100 μg/mL streptomycin, at 37 °C in 5% CO_2. Monolayers of about 104 Vero cells in 96-multiwell plates were treated with several concentrations of the compounds for 72 h. Then, 50 μl of a 1 mg/mL solution of 3-(4,5-dimethylthiazol-2-yl)-2,5-diphenyl tetrazolium bromide (MTT; Sigma) was added to evaluate cell viability according to procedures described elsewhere.[26] The 50% cytotoxic concentration (CC50) was calculated by linear regression analysis of the dose-response curves. All experiments were performed in duplicate at least three times.

Acknowledgments

This study was supported by the following Brazilian agencies and governmental institutions: Fundação Universitária José Bonifácio/Universidade Federal do Rio de Janeiro (FUJB/UFRJ), Coordenação de Aperfeiçoamento de Pessoal de Nível Superior (CAPES), Conselho Nacional de Desenvolvimento Científico e Tecnológico (CNPq), Universidade Federal Fluminense (UFF), and Fundação de Amparo à Pesquisa do Estado do Rio de Janeiro (FAPERJ). Loureiro NI and Rodrigues CR have CNPq fellowships.

References and notes

1. Khan, M. T. H.; Ather, A.; Thompson, K. D.; Gambari, R. *Antiviral Res.* **2005**, *67*, 107–119.
2. Efstathiou, S.; Preston, CM. *Virus Res.* **2005**, *111*, 108–119.
3. D. A. Baker, Management of herpes in pregnancy ACOG: Washington, DC, 1999.
4. De Clercq, E.; Naessens, L.; De Bolle, L.; Schols, D.; Zhang, Y.; Neyts, J. *Rev. Med. Virol.* **2001**, *11*, 381–395.
5. Hayden, F. G. In *The Pharmacological Basis of Therapeutics*; Hardman, J. G., Limbird, L. E., Eds.; McGraw Hill Publisher: NY, 2001; pp 1295–1312.
6. Morfin, F.; Thouvenot, D. J. *Clin. Virol.* **2003**, *26*, 29–37.
7. Chilukuri, S.; Rosen, T. *Dermatol. Clin.* **2003**, *21*, 11–20.
8. Yamamoto, N.; Furukawa, H.; Ito, Y.; Yoshida, S.; Maeno, K.; Nishiyama, Y. *Antiviral Res.* **1989**, *12*, 21–36.
9. Lowden, C. T.; Bastow, K. F. *Antiviral Res.* **2003**, *59*, 143–154.
10. Lowden, C. T.; Bastow, K. F. *J. Med. Chem.* **2003**, *46*, 5015–5020.
11. Akanitapichat, P.; Bastow, K. F. *Antiviral Res.* **2002**, *53*, 113–126.
12. Akanitapichat, P.; Lowden, C. T.; Bastow, K. F. *Antiviral Res.* **2000**, *45*, 123–134.
13. Mello, H.; Echevarria, A.; Bernardino, A. M.; Canto-Cavalheiro, M.; Leon, L. L. J. *Med. Chem.* **2004**, *47*, 5427–5432.
14. Azevedo, A.; Ferreira, V. F.; Mello, H.; Leão-Ferreira, L. R.; Jabor, A. V.; Frugulhetti, I. C. P. P.; Pereira, H. S.; Moussatché, N.; Bernardino, A. M. *Heterocycl. Commun.* **2002**, *8*, 427–432.
15. Bare, T. M.; MacLaren, C. D.; Campbell, J. W.; Firor, J. W.; Resch, J. F.; Walters, C. P.; Salama, A. I.; Meiners, B. A.; Patel, J. B. *J. Med. Chem.* **1989**, *32*, 2561–2573.
16. Azevedo, A. R.; Frugulhetti, I. C. C. P.; Khan, M. A.; Khakwani, S.; Bernardino, A. M. R. *Heterocyclic Communications* **2002**, *8*, 47–54.
17. Khan, M. A.; Rolim, A. M. C. *Monatsh. Chem.* **1983**, *114*, 1079.
18. Lynch, B. M.; Khan, M. A.; C Teo, H.; Pedrotti, F. *Can. J. Chem.* **1988**, *66*, 420–426.
19. Kuo, Y. C.; Chen, C. C.; Tsai, W. J.; Ho, Y. H. *Antiviral Res.* **2001**, *51*, 95–109.
20. Bhattacharjee, A. K.; Majundar, D.; Guha, S. J. J. *Chem. Soc. Perkin Trans.* **1992**, *2*, 805.
21. Politzer, P.; Laurence, P. R.; Jayasuriya, K. *Environ Health Perspect.* **1985**, *61*, 191–202.

22. Bastow, K. F. *Curr. Drug Targets: Infect. Disorders* **2004**, 4323–4330.
23. Bernardino, A. M. R.; Pinheiro, L. C. S.; Rodrigues, C. R.; Loureiro, N. I. V.; Castro, H. C.; Lanfredi-Rangel, A.; Sabatini-Lopes, J.; Borges, J. C.; Carvalho, J. M.; Romeiro, G. A.; Ferreira, V. F.; Frugulhetti, I. C. P. P.; Vannier-Santos, M. A. *Bioorg. Med. Chem.* **2006**, *14*, 5765–5770.
24. Costa, M. S.; Boechat, N.; Rangel, E. A.; da Silva, F. D.; de Souza, A. M.; Rodrigues, C. R.; Castro, H. C.; Junior, I. N.; Lourenco, M. C.; Wardell, S. M.; Ferreira, V. F. *Bioorg. Med. Chem.* **2006**, 8644–8653.
25. Reed, B.; Munch, M. *Am. J. Virol.* **1938**, *27*, 492–504.
26. Mosman, T. *J. Immunol. Methods* **1983**, *65*, 55–63.